

## EXTREME-ULTRAVIOLET EXTINCTION MEASUREMENTS ON HYDROGENATED AND DEHYDROGENATED AMORPHOUS CARBON GRAINS

L. COLANGELI,<sup>1</sup> V. MENNELLA,<sup>2</sup> A. BLANCO,<sup>3</sup> S. FONTI,<sup>3</sup> E. BUSSOLETTI,<sup>2,4</sup> H. E. GÜMLICH,<sup>5</sup>  
 H. C. MERTINS,<sup>5</sup> AND CH. JUNG<sup>6</sup>

Received 1992 March 16; accepted 1993 May 19

### ABSTRACT

We present, for the first time, extinction measurements performed in the extreme-ultraviolet spectral region, down to about 50 nm, on both dehydrogenated and hydrogenated amorphous carbon grains produced in the laboratory. The results evidence a typical extinction feature at 85–95 nm which can be attributed to an active  $\sigma + \pi$  plasmon. This feature is present in all samples we have analyzed, in agreement with the fact that hydrogenation cannot inhibit this kind of resonance. On the other hand, dehydrogenated amorphous carbon particles show an extinction “hump” at around 240–260 nm, which is lacking in the hydrogen-rich sample. In agreement with other authors, we interpret this band in terms of a collective excitation of the  $\pi$  electrons which corresponds to the  $\pi \rightarrow \pi^*$  transition. Present results allow to better characterize the spectral properties of a class of solid particles which have been invoked in various theoretical models of cosmic dust and provide useful hints to interpret the trend of both interstellar and circumstellar extinction curves.

*Subject headings:* circumstellar matter — dust, extinction — stars: carbon — ultraviolet: interstellar

### 1. INTRODUCTION

The spectral features observed both in interstellar and circumstellar extinction curves are one of the main tools to determine the nature of cosmic grains. Extensive studies have allowed us to obtain detailed information about emission bands in the infrared, as well as to differentiate the UV visible spectral profiles detected towards various sources (Massa & Savage 1989). At the same time, new theoretical models of cosmic dust have been proposed (Draine 1989; Mathis & Whiffen 1989; Desert, Boulanger, & Puget 1990) to improve or to substitute previous elaborations (Mathis, Ruml, & Nordsieck 1977; Draine & Lee 1984; Greenberg 1986) and to account for new observational constraints.

Interstellar extinction curves in the UV–far-UV spectral range are characterized by two main features: the so-called bump at 217.5 nm and the curvature in the far-UV. Systematic analyses of astronomical data (Massa, Savage, & Fitzpatrick 1983; Massa & Fitzpatrick 1986; Fitzpatrick & Massa 1986; Massa & Savage 1989) have evidenced the following main characteristics:

- (1) the peak position is stable at 217.5 nm, within 0.8%;
- (2) the values of the bump width are considerably scattered around an average value of 48 nm, within 25%;
- (3) the far-UV rise is poorly related to the shape and intensity of the bump, and it varies from source to source.

Ultraviolet circumstellar extinction characteristics appear quite different from the interstellar profiles. In fact, some sources, such as Abell 30 (Greenstein 1981), R CrB and RY Sgr

(Hecht et al. 1984), and HD 213985 (Buss, Lamers, & Snow 1989) have the UV peak shifted to 230–250 nm. In cases such as  $\alpha$  Sco (Snow et al. 1987) and HD 89353 (Buss et al. 1989) the peak is lacking.

All the above mentioned evidence could indicate that different species have to be invoked to reproduce the observed changes. More likely, the same kind of basic material could be present in different environments; the nature of this material is carbonaceous (Czyzak & Santiago 1973; Yamamoto & Hasegawa 1977; Seki & Hasegawa, 1981; Czyzak, Hirth, & Tabak 1982; Hecht 1986; Buss et al. 1989; Wright 1989). According to theoretical simulations (Hecht 1986; Sorrell 1990), hydrogen content and/or the graphitization degree of submicron amorphous carbon grains could be responsible for the observed peak variations.

Even if the presence of diamond-like particles cannot be excluded a priori (Lewis, Anders, & Draine 1989), theoretical models have attributed the far-UV rise either to scattering from very small grains (Greenberg 1986) or, again, to absorption from amorphous carbon particles (Hecht 1986).

However, the attribution of both UV and far-UV extinction “fingerprints” on the basis of models only is not sufficient to identify the responsible materials. Laboratory spectral analyses of dust-sample analogues of candidate species are necessary to support theoretical computations on an experimental basis. For this reason, our group has recently performed a systematic analysis of the optical properties of both dehydrogenated and hydrogenated submicron amorphous carbon grains at UV wavelengths (Blanco et al. 1991; Colangeli et al. 1992).

The need for extending the knowledge of dust extinction properties even to the extreme-UV (EUV) has been strongly pointed out at the first Extreme Ultraviolet Astronomy Berkeley Colloquium (Malina & Bowyer 1991). In fact, today it appears clear that the interstellar medium, at wavelengths between the Lyman limit (912 Å) and the X-ray region, is not totally opaque, despite the effective absorption of hydrogen and helium elements. In addition, a careful determination of the dust extinction properties in the EUV is very important, as

<sup>1</sup> Dipartimento di Ingegneria Industriale, University of Cassino, Via Zamosch 43, I-03043 Cassino (FR), Italy

<sup>2</sup> Osservatorio Astronomico di Capodimonte, Via Moiariello 16, I-80131 Napoli, Italy

<sup>3</sup> Physics Department, University of Lecce, Via per Arnesano, I-73100 Lecce, Italy

<sup>4</sup> Istituto di Fisica Sperimentale, Istituto Universitario Navale, Via A. De Gasperi 5, I-80133 Napoli, Italy

<sup>5</sup> Technical University of Berlin, Institut für Festkörperphysik, Sekr. PN 4-1, Hardenbergstrasse 36, D-1000 Berlin, Germany

<sup>6</sup> BESSY GmbH, Lentzeallee 100, D-1000 Berlin, Germany

they can be used as input to theoretical models devoted to the interpretation of the observed Galactic far-IR background (Hawkins & Wright 1991 and references therein).

In this paper we report, for the first time, EUV extinction data for amorphous carbon grains produced by homogeneous condensation both in inert (Ar) and in hydrogen-rich ( $H_2$ ) environments. The use of an experimental technique different from that used in our previous measurements allowed us to extend the spectroscopic investigation of carbon grains down to about 50 nm. The measurements were performed at the BESSY (Berliner Elektronenspeicherring-Gesellschaft für Synchrotronstrahlung GmbH) synchrotron light facility in Berlin. Present data allow us to better characterize the UV-far-UV spectral properties of both dehydrogenated and hydrogenated amorphous carbon grains. It is now possible to interpret the extinction rise in the far-UV, already observed in previous measurements (Colangeli et al. 1992), as the low energy tail of a broad peak falling between 85 and 95 nm.

In § 2 we describe both the conditions of production for the examined samples and the experimental setup used for the present measurements. In § 3 we discuss the optical characteristics of the samples analyzed in the spectral range 50–300 nm. Finally, in § 4 we interpret our results on the basis of both theoretical background and previous laboratory data. The complete set of spectral data reported here allows us to provide an interpretation of the interstellar and circumstellar extinction curves.

## 2. EXPERIMENTAL

The amorphous carbon grains studied in this work were prepared by arc discharge (AC samples) and by benzene burning in air (BE samples)—see Bussoletti et al. 1987 for further details about production techniques. The arc discharge occurred between two amorphous carbon electrodes in argon (AC-AR sample) and hydrogen (AC-H2 sample), at a pressure of 10 mbar. The BE sample were produced in air at room conditions.

In the present experiment the dust was collected at a distance of 5 cm from the source. As already reported by Borghesi et al. (1983) and Blanco et al. (1991), round-shaped grains forming “fluffy” structures were produced; AC-AR and AC-H2 particles have similar sizes (average radius  $\langle a \rangle \simeq 40$  Å), while BE grains are larger ( $\langle a \rangle \simeq 150$  Å). The amorphous status of the samples is confirmed by the lack of spots or fringes in their diffraction patterns.

In previous measurements (Colangeli et al. 1986, 1992) the dust samples were deposited onto lithium fluoride windows, whose typical cutoff is around 105 nm. In order to extend the spectral range shortward, for the present measurements we adopted a different technique. The substrate used to collect the dust was gold-coated quartz. Only half of the surface was covered with grains, in order to measure also the optical properties of the gold.

The procedure used to perform the present measurements is schematically sketched in Figure 1, and it consists of the following two phases. In the first step the incident monochromatic beam is focused on the half-portion of the substrate covered with dust, while in the second step the same procedure is repeated for the clean half of the substrate. The intensity of both the incident beam,  $I_{in}$  and  $I'_{in}$ , and of the outgoing beam,  $I_{out}$  and  $I'_{out}$ , is measured for the two cases. The angle formed by the incident beam with the normal direction to the sample is  $5^\circ \pm 2^\circ$ .

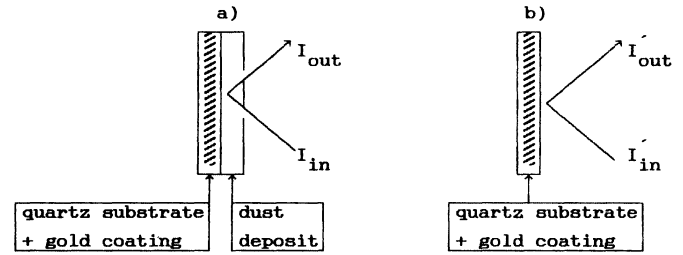


FIG. 1.—Steps of measurements used to determine the transmittance of the dust samples deposited onto the gold mirrors (see text). (a) Measurement on the half of the substrate covered by dust; (b) measurement on the clean half of the substrate.

The synchrotron light from the BESSY storage ring (energy  $\simeq 800$  MeV; current = 500–100 mA) was analyzed by a 3 m normal incidence monochromator and focused (beam size  $\simeq 2$  mm<sup>2</sup>) onto the samples. The whole spectral range from 300 to 50 nm was divided in different subintervals by using two different gratings (see Table 1). Two filters were used to suppress the higher orders’ contribution to the spectra: quartz suprasil filter (cutoff is 160 nm) and a lithium fluoride filter (cutoff is 105 nm).

The radiation was detected by a photomultiplier coupled with a sodium salicylate filter. After amplification, the signal was converted in digital form and stored in an “on-line” computer. To monitor both  $I_{in}$  (or  $I'_{in}$ ) and  $I_{out}$  (or  $I'_{out}$ ) a 45° rotating mirror was synchronized both with the monochromator and the signal acquisition system in order to detect the two incident and outgoing signals alternatively at each wavelength step.

By using the previous method, our measurements were limited only by the reflectivity of the gold substrate, which does not present sharp features in the EUV spectral region.

## 3. RESULTS

According to the experimental setup described in the previous section, the intensity  $I_{out}$  measured for the dust + substrate system should be given by

$$I_{out} = I_{in} T_{dust}^2 R_{gold} \quad (1)$$

(see Fig. 1), where  $R_{gold}$  is the reflectivity of the gold substrate and  $T_{dust}$  is the transmittance of the dust. On the other hand, for the clean half of the substrate we obtain

$$I'_{out} = I'_{in} R_{gold} \quad (2)$$

From equations (1) and (2) we obtain

$$T_{dust} = \left( \frac{I_{out}/I_{in}}{I'_{out}/I'_{in}} \right)^{1/2} \quad (3)$$

We observe that the transmittance data computed by using equation (3) match perfectly with the results previously obtained in the 300–110 nm wavelength range by means of the standard transmittance technique (Colangeli et al. 1992).

TABLE 1  
SPECTRAL RANGES ANALYZED IN OUR MEASUREMENTS

Range (nm)	Step (nm)	Grating	Filter
300–150 .....	0.5	Al (600 1 mm <sup>-1</sup> )	Quartz suprasil
200–100 .....	0.5	Al (600 1 mm <sup>-1</sup> )	LiF
120–50 .....	0.2	Al (600 1 mm <sup>-1</sup> )	None
120–50 .....	0.2	Pt (1200 1 mm <sup>-1</sup> )	None

We have to recall here that, according to the classic electromagnetic theory, a nontrivial boundary-value problem is faced near the surface of the substrate covered with dust, owing to the interaction between incident and reflected waves, on a length scale smaller than or comparable to the wavelength of the radiation. Then equation (1) could give a simplified view of the actual physical process. On the other hand, transmission (Borghesi et al. 1983; Blanco et al. 1991) and new scanning electron microscopy measurement show that our grains are arranged in loosely clustered, "fluffy" aggregates, so that they form on the gold-coated substrate a layer several times thicker than the EUV light wavelengths. Therefore, the outgoing intensity should be affected only slightly by the processes occurring at the boundary with the substrate and, although approximated, equation (1) should be applicable to our conditions. The agreement of present results with previous transmittance data (Colangeli et al. 1992) in the 300–110 nm wavelength range seems to confirm our interpretation.

Moreover, we have to notice that (a) as the wavelength decreases, boundary effects should be limited at an even thinner layer of the dust deposit and then should become more and more negligible and that (b) the measured reflectance of the gold coating at  $\lambda < 110$  nm appears smoother than at longer wavelengths (where equation [3] gives results in agreement with transmittance measurements). Therefore, we tend to exclude that either boundary effects or the optical properties of the gold-coated substrate can affect the results obtained from the application of equation (3) also at wavelengths shorter than 110 nm.

It is useful to mention, here, that the samples analyzed in the present study have been prepared taking into account the results of previous transmittance measurements reported in Colangeli et al. (1992) for similar carbon grains. In that paper the influence of various boundary experimental conditions on the extinction profiles of carbon grains was studied. In particular, the transmittance level at around 250 nm,  $T(250 \text{ nm})$ , where a well pronounced extinction peak falls, was used as an indicator of the dust amount collected per unit area on lithium fluoride windows. It was shown that for  $T(250 \text{ nm})$  in the range 25%–80%, i.e., for different dust amounts, the extinction profiles did not change significantly. In order to work under similar conditions, in the present experiment the dust deposit onto gold substrate was controlled in order to have a total transmittance  $T(250 \text{ nm}) \geq 50\%$ . This procedure allowed us to obtain a transmittance larger than about 40% over all the examined spectral range and therefore an optical depth smaller than 1.

The transmittance data computed by using equation (3) have been used to obtain the normalized extinction curves reported in Figure 2. These spectra are the result of an averaging process of different measurements on each of the three samples (AC-AR, AC-H2, and BE). The uncertainty on the wavelength is about  $\pm 3 \text{ \AA}$ , while the random errors on the normalized extinction data are smaller than 5%.

The analysis of the spectra reported in Figure 2 allows us to identify the following main features:

- (1) a "bump" falling at  $\lambda_p \approx 240$  nm in the spectrum of AC-AR sample and at  $\lambda_p \approx 260$  nm for BE, respectively; the "bump" is absent in AC-H2;
- (2) a minimum in the extinction around  $\lambda_M = 170$  nm for both AC-AR and BE;
- (3) a peak falling at  $\approx 85$  nm for AC-AR and AC-H2 and at  $\approx 95$  nm for BE samples.

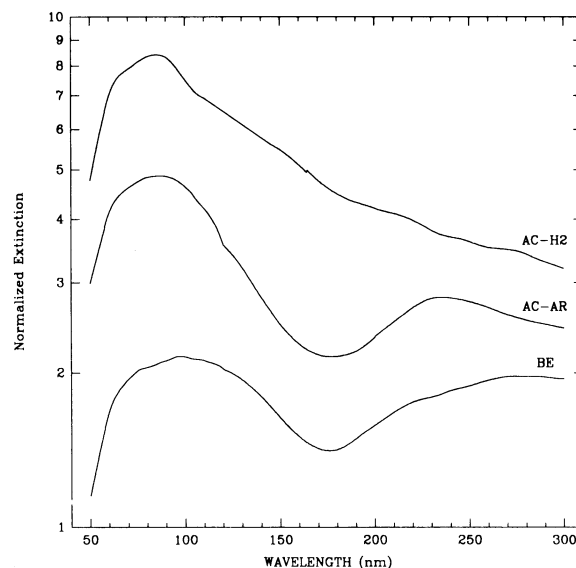


FIG. 2.—Normalized extinction spectra measured on AC-H2, AC-AR, and BE samples. The spectra are arbitrarily shifted in extinction. The uncertainty on wavelength is  $\pm 3 \text{ \AA}$ , while the random errors on the data are smaller than 5%.

In addition, the extinction ratio of the two peaks is different for AC-AR and BE samples, respectively. In fact,  $[E(85 \text{ nm})/E(240 \text{ nm})](\text{AC-AR}) \approx 1.7$ , while  $[E(95 \text{ nm})/E(260 \text{ nm})](\text{BE}) \approx 1.1$ , where  $E(\lambda)$  is the extinction at wavelength  $\lambda$ .

Colangeli et al. (1992) have reported for AC-AR and BE dust samples UV peak positions consistent with the present results. Moreover, their suggestion that the rise in extinction observed from 170 to 100 nm was due to a second peak falling in the far-UV region is definitely confirmed by present data. Blanco et al. (1991) have already reported that amorphous carbon grains produced in  $\text{H}_2$  ambient do not show any hump and produce a progressively rising extinction in the far-UV. For this kind of sample, too, we confirm the absence of the UV peak, and we can presently assess that the far-UV rise is the low-energy wing of a peak falling around 85 nm.

#### 4. DISCUSSION AND CONCLUSIONS

To the best of our knowledge, present data are the first extinction laboratory measurements on submicron carbon grains at wavelengths shorter than 105 nm. The results indicate the presence of a relevant peak in the range 85–95 nm. Following Fink et al. (1984), who analyzed hydrocarbon-plasma-generated carbon films, we tend to attribute the feature to an active  $\sigma + \pi$  plasmon. It is important to note that we observe the band in all the samples analyzed, in agreement with the fact that hydrogenation cannot inhibit this kind of resonance (Hecht 1986). However, according to Fink et al. (1984), the hydrogen content, as well as the density of the sample, can strongly influence the actual position of the EUV peak. In our case, the difference in the peak position between BE ( $\approx 95$  nm) and the other two samples ( $\approx 85$  nm) could be due to such an effect.

As far as the long-wavelength ( $\lambda > 105$  nm) part of our spectra is concerned, we have to observe that, in agreement with previous results (Huffman 1977; Stephens 1980; Koike, Hasegawa, & Manabe 1980; Borghesi, Bussolotti, & Colangeli 1985; Colangeli et al. 1986, 1992), AC-AR and BE samples



show the “hump” falling around 240 and 260 nm, respectively. As already discussed in previous papers (see, for instance, Colangeli et al. 1992 and references therein), this UV resonance arises from collective excitation of the  $\pi$  electrons and corresponds to the  $\pi \rightarrow \pi^*$  transition (Gilra 1971; Fink et al. 1984).

Blanco et al. (1991) have interpreted the lack of the feature in the extinction spectrum of amorphous carbon grains produced in  $H_2$  atmosphere in terms of localization of the  $\pi$  electrons, with subsequent reduction of the collective  $\pi$  resonance, owing to the hydrogenation of the carbon. This behavior was predicted on the basis of theoretical analyses (Hecht 1986; Sorrell 1990), and it was also observed experimentally in hydrogen-containing carbon films (McKenzie et al. 1983; Fink et al. 1984). We have to stress that both the shape and the mean size of the AC-AR and AC-H2 grains are quite similar; therefore, no morphological effect can be invoked to account for the measured differences in extinction between the two samples.

Size effects could be responsible for the difference in peak position observed for AC-AR and BE samples (Perenboom, Wyder, & Meier 1981; Genzel, Martin, & Kreibig 1975; Wickramasinghe, Lukes, & Dempsey 1974; Wickramasinghe & Nandy 1974), as these grains have mean radii of 40 Å and 150 Å, respectively. On the other hand, according to Hecht (1986), a short-scale graphitization of the “disordered” grains can produce a shift of the plasmon resonance. Therefore, at least size effects and graphitization could contribute to determine the actual peak position. At present, it does not seem possible to choose among the mentioned possibilities, and further measurements are needed to better characterize the properties of the examined particles. For example, NMR and/or Extended X-ray absorption fine structure (EXAFS) techniques (Robertson 1986) may give further hints about the carbon orbital hybridization ratio  $sp^2/sp^3$  (i.e., graphite-like vs. diamond-like) and may help to solve some of the open questions.

At this point we have to recall that, as evidence in Transmission Electron Microscopy (TEM) and Scanning Electron Microscopy (SEM) images, the grains deposited onto the gold substrates form aggregates of particles which are in physical contact. Therefore, clustering effects could influence the measured optical properties. As already mentioned in § 3, Colangeli et al. (1992) have shown experimentally that the UV-optical properties of AC-AR grains do not vary significantly for various amounts of dust mass collected onto the substrate. This result should indicate that our results are independent from large-scale clumping effects. On the other hand, the computations performed by Wright (1989), and based on the theoretical “graphitic onion” model, show that the UV peak already shifts from 204 nm, for a single grain, to 240 nm, for aggregates of four or eight spheres. According to the previous model, the bump in our spectra could be shifted at wavelengths longer than 220 nm as a consequence of the “clustering.”

Nevertheless, we tend to exclude the hypothesis that the spectral changes observed for samples produced under various conditions could be due to clustering differences rather than to the intrinsic properties of the carbon grains. In fact, in a very recent paper Blanco et al. (1992) have shown that the lack of the UV peak around 240 nm in AC-H2 samples is related to hydrogenation rather than morphological properties of the grains. Experiments have demonstrated that after annealing, i.e., after the hydrogen is removed, the UV peak is restored, while TEM images show no change both in the morphology

and in the agglomeration degree of the grains. Therefore, it is likely that the appearance or the lack of the UV peak is related to the hydrogen content of the carbon samples.

It also appears useful to compare present data with the output of theoretical computations, which are frequently used for astronomical applications. For this purpose, we have used the optical constants, available in the literature for some representative carbonaceous materials, to compute the extinction factor of monosized ( $a = 0.01 \mu\text{m}$ ) spherical grains by means of the Mie theory. In particular, we have considered (1) the “interstellar graphite” theoretically synthesized by Draine & Lee (1984) and Draine (1985); (2) the hydrogenated amorphous carbon film produced by Duley (1984); and (3) the so-called glassy carbon analyzed by Williams & Arakawa (1972).

The comparison of the experimental data with the theoretical results is reported in Figure 3. We can observe that

- (1) the spectral profile of AC-H2 grains fits reasonably well the spectrum computed for hydrogenated amorphous carbon;
- (2) the peak positions of the AC-AR sample are in good agreement with those of “glassy” carbon;
- (3) the EUV peak of “interstellar” graphite matches the position observed in our measurements for both AC-AR and AC-H2 samples.

It is, however, evident that the measured band profiles are quite broader than those obtained with Mie computations. This is not surprising, as theoretical results pertain to monosized, well isolated, and perfectly spherical grains (Bohren & Huffman 1983). On the contrary, the measured spectral profile of the extinction peak falling around 85 nm is quite similar to that computed by Hawkins & Wright (1991) for an amorphous carbon fractal dust grain made of 64 “monomers,” each one with a radius of 25 Å (see their Fig. 6).

Let us now discuss the influence of our experimental results on the interpretation of astronomical ultraviolet spectra. Our

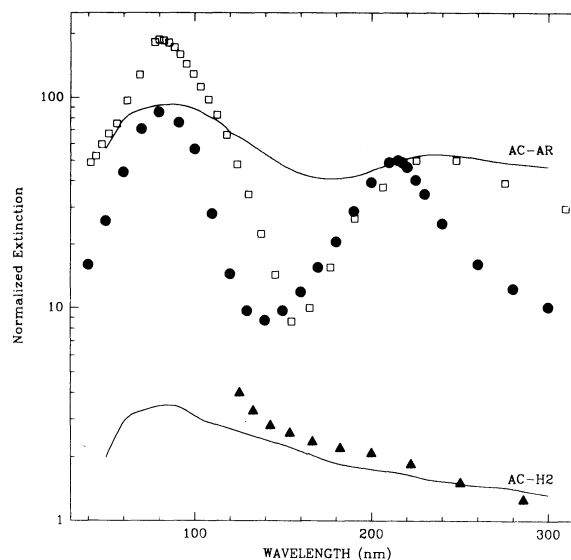


FIG. 3.—Comparison of our data (solid lines) with the extinction efficiencies computed for monosized ( $a = 0.01 \mu\text{m}$ ) spherical grains by means of the Mie theory. The optical constants used for the computations are from Duley (1984) for hydrogenated amorphous carbon (triangles), from Draine (1985) for “interstellar” graphite (dots), and from Williams & Arakawa (1972) for “glassy” carbon (open squares). The curves are arbitrarily shifted in extinction for comparison.

data appear in line with the model proposed by Hecht (1986) and further developed by Sorrell (1990). As confirmed by our spectra, the hydrogenation degree of carbonaceous grains may play a major role in the appearance of the UV "bump." Hydrogenated amorphous carbon grains (AC-H2) do not exhibit any UV feature, while dehydrogenated particles (AC-AR) show a typical 240 nm extinction peak. These two classes of grains could explain the extinction curves observed in circumstellar environments, where the peak is sometimes absent—i.e.,  $\alpha$  Sco (Snow et al. 1987) and HD 89353 (Buss et al. 1989)—or observed around 240 nm—i.e., Abell 30 (Greenstein 1981), R CrB and RY Sgr (Hecht et al. 1984), and HD 213985 (Buss et al. 1989). This suggestion is based also on the following evidences: (1) carbonaceous grains ejected by carbon stars are amorphous (Hecht et al. 1984; Martin & Rogers 1987; Rowan-Robinson et al. 1986) and (2) Abell 30, for example, is classified as a hydrogen-poor planetary nebula (Greenstein 1981).

Following Hecht (1986) and Sorrell (1990), in order to reproduce the interstellar peak at 217.5 nm it is necessary to assume that Rayleigh-size amorphous carbon grains are processed by UV irradiation, once in the interstellar medium.

Our laboratory results may also have a significant impact on the interpretation of the steep rise toward the far-UV observed in the extinction curves. It is clear that amorphous carbon grains, similar to those analyzed in our experiment, can contribute substantially to the far-UV extinction rise observed in circumstellar envelopes of carbon-rich stars, whether or not the particles are hydrogenated or dehydrogenated. In fact, such a rise should represent the long-wavelength wing of a peak falling around 85–95 nm.

Furthermore, our experimental results evidence that when both the EUV peak and the UV "bump" are present, their relative intensity may vary from sample to sample. According to Fink et al. (1984), this effect can be related to the hydrogenation and/or to the graphitic content of the samples. Therefore, the combined study of the "bump" intensity and of the

far-UV curvature of the interstellar extinction curves could be a further tool to determine the chemical and structural properties of carbonaceous grains in different environments.

On the other hand, according to the theoretical computations performed by Hawkins & Wright (1991) for fractal dust grains, the silicate extinction cross section also rises in the far-UV and peaks at about 79 nm. Therefore, it appears rather difficult to attribute either to the carbonaceous or to the silicate components the observed spectral profiles; thus, it seems reasonable that both two classes of grains can contribute to this behavior of the extinction curve.

Astronomical observations at wavelengths shorter than the Lyman limit (912 Å) are currently lacking. In fact, the most abundant elements in the universe, hydrogen and helium, provide most of the opacity in the EUV. However, according to Malina & Bowyer (1991), there is some chance that future space-borne observations will provide information about the extinction of the dust component, at least towards gas-free regions. The comparison of astronomical data with the experimental results reported in the present paper may be, then, a further valuable diagnostic tool to identify the actual composition of cosmic dust.

Finally, the present extinction data in the EUV will be useful in the interpretation of the observed galactic far-IR background (Hawkins & Wright 1991 and references therein). In fact, the conversion of starlight into thermal radiation by dust grains is the main cause of the emission background in the diffuse medium, and the efficiency of this process is strongly related to the optical properties of solid particles at short wavelengths. The data reported in this paper can be used as input to theoretical models devoted to the simulation of far-IR astronomical observations.

This work has been supported under the European Community, Large Scale Installations Program, Contract GE 1-0018-D(B) and by ASI, CNR, and MURST.

## REFERENCES

- Blanco, A., Bussoletti, E., Colangeli, L., Fonti, S., Mennella, V., & Stephens, J. R. 1992, *ApJ*, 406, 739
- Blanco, A., Bussoletti, E., Colangeli, L., Fonti, S., & Stephens, J. R. 1991, *ApJ*, 382, L97
- Bohren, C. F., & Huffman, D. R. 1983, *Absorption and Scattering of Light by Small Particles* (New York: Wiley)
- Borghesi, A., Bussoletti, E., & Colangeli, L. 1985, *A&A*, 142, 225
- Borghesi, A., Bussoletti, E., Colangeli, L., Minafra, A., & Rubini, F. 1983, *Infrared Phys.*, 23, 85
- Buss, R. H., Lamers, H., & Snow, T. P. 1989, *ApJ*, 347, 977
- Bussoletti, E., Colangeli, L., Borghesi, A., & Orofino, V. 1987, *A&AS*, 70, 257
- Colangeli, L., Blanco, A., Fonti, S., & Bussoletti, E. 1992, *ApJ*, 392, 284
- Colangeli, L., Capozzi, V., Bussoletti, E., & Minafra, A. 1986, *A&A*, 168, 349
- Czyzak, S. J., Hirth, J. P., & Tabak, R. G. 1982, *Vistas Astron.*, 25, 337
- Czyzak, S. J., & Santiago, J. J. 1973, *Ap&SS*, 23, 443
- Desert, F.-X., Boulanger, F., & Puget, J. L. 1990, *A&A*, 237, 215
- Draine, B. 1985, *ApJS*, 57, 587
- Draine, B. D. 1989, in *Interstellar Dust*, ed. L. J. Allamandola & A. G. G. M. Tielens (Dordrecht: Kluwer), 313
- Draine, B., & Lee, H. M. 1984, *ApJ*, 285, 89
- Duley, W. W. 1984, *ApJ*, 287, 694
- Fink, J., Müller-Heinzerling, T., Pfüger, J., Scheerer, B., Dischler, B., Koidl, P., Bubenzer, A., & Sah, R. 1984, *Phys. Rev. B*, 30, 4713
- Fitzpatrick, E. L., & Massa, D. 1986, *ApJ*, 307, 286
- Genzel, L., Martin, T. P., & Kreibig, U. 1975, *Z. Phys. B*, 21, 339
- Gilra, D. P. 1971, *Nature*, 299, 237
- Greenberg, J. M. 1986, in *Light on Dark Matter*, ed. F. P. Israel (Dordrecht: Reidel), 177
- Greenstein, J. L. 1981, *ApJ*, 245, 124
- Hawkins, I., & Wright, E. L. 1991, in *Extreme Ultraviolet Astronomy*, ed. R. F. Malina & S. Bowyer (New York: Pergamon), 333
- Hecht, J. 1986, *ApJ*, 305, 817
- Hecht, J., Holm, A. V., Donn, B., & Wu, C.-C. 1984, *ApJ*, 280, 228
- Huffman, D. R. 1977, *Adv. Phys.*, 26, 129
- Koike, C., Hasegawa, H., & Manabe, A. 1980, *Ap&SS*, 67, 495
- Lewis, R. S., Anders, E., & Draine, B. T. 1989, *Nature*, 339, 117
- Malina, R. F., & Bowyer, S., ed. 1991, *Extreme Ultraviolet Astronomy* (New York: Pergamon)
- Martin, P. G., & Rogers, C. 1987, *ApJ*, 322, 374
- Massa, D., & Fitzpatrick, E. L. 1986, *ApJS*, 60, 305
- Massa, D., & Savage, B. 1989, in *Interstellar Dust*, ed. L. J. Allamandola & A. G. G. M. Tielens (Dordrecht: Kluwer), 3
- Massa, D., Savage, B. D., & Fitzpatrick, E. L. 1983, *ApJ*, 266, 662
- Mathis, J. S., Rimpl, W., & Nordsieck, K. H. 1977, *ApJ*, 217, 425
- Mathis, J. S., & Whiffen, G. 1989, *ApJ*, 341, 808
- McKenzie, D. R., McPhedran, R. C., Savvides, N., & Cockayne, D. J. H. 1983, *Thin Solid Films*, 108, 247
- Perenboom, J. A. A. J., Wyder, P., & Meier, F. 1981, *Phys. Rep.*, 78, 173
- Robertson, J. 1986, *Adv. Phys.*, 35, 317
- Rowan-Robinson, M., Lock, T. D., Walker, D. W., & Harris, S. 1986, *MNRAS*, 222, 273
- Seki, J., & Hasegawa, H. 1981, *Prog. Theor. Phys.*, 66, 903
- Snow, T. P., Buss, R. H., Gilra, D. P., & Swings, J. P. 1987, *ApJ*, 321, 921
- Sorrell, W. H. 1990, *MNRAS*, 243, 570
- Stephens, J. R. 1980, *ApJ*, 237, 450
- Wickramasinghe, N. C., Lukes, T., & Dempsey, M. J. 1974, *Ap&SS*, 30, 315
- Wickramasinghe, N. C., & Nandy, K. 1974, *Ap&SS*, 26, 123
- Williams, M. W., & Arakawa, E. T. 1972, *J. Appl. Phys.*, 43, 2460
- Wright, E. L. 1989, *ApJ*, 346, L89
- Yamamoto, T., & Hasegawa, H. 1977, *Prog. Theor. Phys.*, 58, 816